URSI-B EMTS 2025, Bologna, 23–27 June

Innovative Application of the Born-Approximation for Analyzing Medium Motion Effects in COMSOL Time Explicit EMW Module

Kirill Zeyde*[(1)] and Mirco Raffetto[(1)]
(1) University of Genoa, Genoa, Italy, https://unige.it

Abstract

This article presents an algorithm for integrating a previously developed methodology into the COMSOL Time Explicit EMW Module. The Born Approximations were applied to analyze medium motion effects, equivalent to weak bianisotropy. These effects are challenging to calculate precisely due to their low magnitude relative to computational noise in classical approaches. Integration into CAD enables broader and more effective application. Validation is provided for a 2.5D problem of axial motion of a circular cylinder, demonstrating excellent agreement with the results.

1 Introduction

In this article, we examine a specific algorithm for integrating the methodology we previously developed (a full description of the methodology is available in [1]) into a commercial environment for further numerical investigations. The Born Approximations (BAs) were used to analyze the effects of medium motion, which are equivalent to the effects of weak bianisotropy. A precise analysis of such effects is significantly complicated due to their low magnitude against the background of computational noise, when using classical computational approaches.

A notable advantage of the methodology we developed is its flexibility for implementation using well-known professional software. The ability to describe an electromagnetic source as a distribution of electric and magnetic current densities is both necessary and sufficient. The commercial CAD software, COMSOL Multiphysics, provides this capability. Incorporating BAs into this modeling environment, along with the generality of the approach, opens up a wide range of possibilities. The developed methodology not only addresses the theoretical challenge of analyzing the very weak effects of medium motion (see, *e.g.* [1, 2]), but its integration into COMSOL is also of significant practical interest. The capability to perform multiscale and multiphysics simulations, as well as parametric optimization over arbitrary geometries, allows for the solution of problems that previously lacked reliable solutions. This is especially relevant for the development of devices based on the weak bianisotropy effects of the medium, such as flowmeters and profilers for liquids or gases [3, 4, 5], as well as for dielectric spectroscopy and material structuroscopy [6, 7, 8]. It is also worth highlighting the potential for efficient solutions to inverse problems in various applications [1, 9, 10]. The approach described in this paper involves modular modeling [11], which significantly enhances the capabilities of the new methodology when applied to commercial software. We also explored the potential for integrating our methodology for analyzing weak bianisotropy effects into other professional electromagnetic modeling systems. However, the simplicity of the combination algorithm and the performance of the solver, along with the new opportunities arising from this integration, position CAD COMSOL as the most advantageous option.

It is important to note that the authors have developed their own finite element solver, referred to as 'native.' This methodology has been verified against analytical solutions for 2.5D problems [1] and partially for 3D problems [2]. Several publications discuss the performance of the native finite element solver in various scenarios (see, *e.g.*, [10, 12, 13]). One apparent advantage of using the native solver is the ability to maintain complete control over the computational kernel processes. However, certain operational constraints—such as solver performance, parametric optimization, and mesh generation capabilities—limit the general applicability of this approach. Integrating the methodology into a commercial system effectively addresses these limitations. At the same time, the native solver remains the most effective tool for comprehensive validation of new numerical analysis methods and approaches.

2 General Workflow

Fig. 1 shows a diagram of the main processes for applying the methodology in COMSOL. It is important to note that while we use the native solver here to obtain equivalent currents, there are no restrictions for the user in this context. Equivalent source currents can be obtained using any available and convenient method. The second stage is merely converting the output data format of the equivalent sources to a format that can be imported into COMSOL. The subsequent operations are described later in the text.

The calculation of equivalent sources is described in detail in [1]. Different approaches in describing the parameters of the bianisotropy medium, are outlined in the [14, 15].

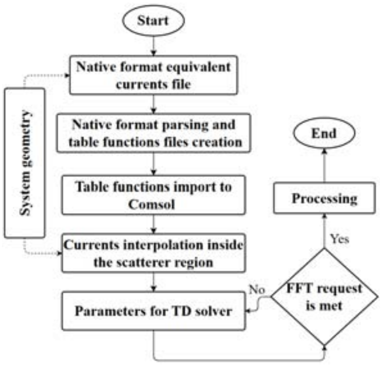

Figure 1. Workflow diagram for applying the methodology with COMSOL Multiphysics.

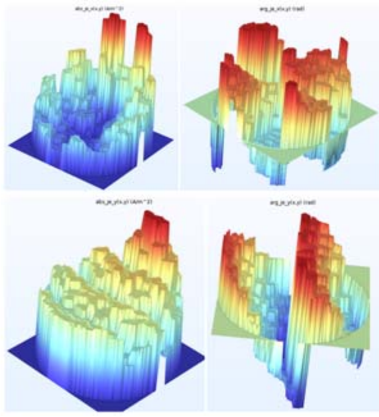

Figure 2. Example of interpolation of some components of the electrical equivalent current densities in COMSOL. Top left for $|J_x(x,y)|$, top right for $\arg[J_x(x,y)]$, bottom left for $|J_y(x,y)|$ and bottom right for $\arg[J_x(x,y)]$.

Both of these works are essential for realizing the equivalent transition in general and for integrating the Born approximation into the COMSOL environment, in particular. It is important to note that the proposed approach eliminates the need for numerical calculations of a bianisotropic medium (which are often challenging [10, 16, 17]). This is a distinctive general feature of the method, which becomes even more efficient when implemented in powerful CAD.

To simplify the objective formulation, we need to describe the source of electromagnetic waves in the system using the distribution of electric and magnetic currents [18]. We utilize the "Electromagnetic Waves, Time Explicit" COMSOL module with the "Time to Frequency FFT" predefined study step. In this module, it is possible to define time-dependent sources of both types of currents (electric and magnetic). However, the distribution of magnetic currents cannot be described over the domain in the frequency domain solver in COMSOL [19].

In the time domain (TD), the harmonic current sources oscillations are written as follows:

$$\begin{aligned}\mathbf{J}(x,y,z) = &|J_x(x,y,z)| \times cos(\omega t + \arg[J_x(x,y,z)])\hat{x} + \\ &|J_y(x,y,z)| \times cos(\omega t + \arg[J_y(x,y,z)])\hat{y} + \\ &|J_z(x,y,z)| \times cos(\omega t + \arg[J_z(x,y,z)])\hat{z}.\end{aligned} \quad (1)$$

This applies to the complex amplitudes of the sources defined in the frequency domain for both electric and magnetic currents. Using the principles of finite element approximation, we determine the values of currents at the centres of gravity of the elements. Consequently, mesh refinement contributes to an improved description of the source current distribution. This approach is conceptually similar to another equivalent description of the moving medium through the coordinate dependence of the propagation constant [20].

A table-defined function is created to describe expression (1), which establishes the standard intrinsic COMSOL interpolation procedure. The first columns contain the coordinates of the points (x, y, and/or z), while the subsequent column contains the phase or magnitude values of the corresponding current component. Thus, according to (1), a total of 12 files are loaded into COMSOL in the general case (6 for electric currents and 6 for magnetic currents). Once the data is loaded into COMSOL, the internal interpolation algorithm can be any method (nearest neighbor or linear). The quality of interpolation, where the current within a single element is constant (nearest neighbor), depends solely on the loaded files. Extrapolation should adhere to a predetermined rule: it must take a value strictly equal to zero outside the defined domain of the currents. As an illustrative example, Fig. 2 shows the distributions of electrical equivalent currents imported into COMSOL to describe function (1). The parameters used to obtain these distributions correspond to those under which the validation results are presented in Section 4.

3 Time Domain Transition

The problem is initially formulated in TD, after which the classical fast Fourier transform (FFT) is applied to obtain the desired result in the frequency domain. We begin by introducing three key time values: $T = \frac{1}{f}$, $T_t = \frac{s}{v_p}$ and T_{obs}. Here, T represents the period of the oscillations of interest, T_t is the travel time for the wave to propagate from the source to the boundary of the numerical domain, and T_{obs} is the observation time. These three time values are related by the inequality: $T < T_t < T_{obs}$. This means that during the observation of the periodic process, the wave from the source (1) must reach the observer (located at the boundary of the numerical analysis domain) while completing several full oscillation periods. Otherwise, there will not be enough information to restore the characteristics of the process of interest.

Next, we define the frequency discretization as $d_f = \frac{f}{n_f}$, where n_f is a number of frequencies steps. The observation time is then related to this value as $T_{obs} = \frac{1}{d_f}$. Hence the obvious conclusion $\frac{T_{obs}}{T} = n_f > 1$ immediately follows. Analogously we have to define the temporal discretization. First, $d_t = \frac{T_{obs}}{n_s}$, where n_s is the number of samples. Second, sampling frequency is $f_s = \frac{1}{d_t}$. According to the Nyquist–Shannon theorem, $f_s > 2f$ must be strictly satisfied. This condition leads us to the inequality $1 < n_f < \frac{n_s}{2}$. The physical meaning of the introduced quantities is standard when observing a periodic process for a limited period of time. Thus, n_f is the number of periods during the observation, n_s is the number of reports during the observation, hence $n_{rep} = \frac{n_s}{n_f}$ is the number of reports per period. In this context by reports we mean the record of the oscillatory process parameters of state [19].

For the output time settings, we use a set of reports within the interval $[0 \div T_{obs}]$ with a step size equal to d_t. We apply continuous Fourier transformation scaling over the interval $[0 \div T_{obs}]$, where f represents the maximum output frequency. Since n_f is an input parameter, it is always an integer, which ensures the inclusion of the frequency f in the output Fourier spectrum.

4 Numerical Results and Verification

The BA methodology from [1] was validated for the 2.5D case by comparing it with the analytical solution [21], using the native solver for a classical electromagnetic scattering problem involving a moving circular cylinder. The native solver's results are considered a reliable reference, with accuracy sometimes surpassing traditional analytical methods (see [1, 2]). This enhanced accuracy is attributed to the BA methodology, not just the native solver. We expect similar or even improved results in COMSOL, which we will verify by applying the methodology to this well-established problem.

The geometry of this problem matches that presented in [1], as well as the analytical solutions in [21, 22]. Scatterer region is a disk with its center coinciding with the center of the numerical analysis domain. The outer boundary of the numerical domain is subject to scattering boundary conditions, with a constant impedance of Z_0. The background medium is free space. Incident wave frequency $f = 1$ GHz; numerical domain radius $R = 2.968$ m; radius of scatterer $r = 0.211$ m; permittivity of scatterer $\varepsilon_r = 2$; non-magnetic. Both the native solver and COMSOL use the same computational mesh, which was generated by COMSOL's standard mesh generator for the reference frequency of $2f$. The following parameters were selected for the time-domain solver: $n_s = 512$ and $n_f = 200$, resulting in an observation time of $T_{obs} = 2 \times 10^{-7}$ s. To determine the wave travel time, T_t, we note that the shortest path from the source region to the boundary of the numerical domain is $(R - r)$. Since the wave propagates at the speed of light, the travel time is approximately $T_t \approx 9.2 \times 10^{-9}$ s. Given that the oscillation period of the source is $T = 10^{-9}$ s, the fundamental time inequality is strictly satisfied. For validation purposes, we use the smallest residual value to terminate the iterative process in the native solver, i.e., $\delta = 10^{-12}$. A more detailed description of the solver's operation can be found in [1, 13].

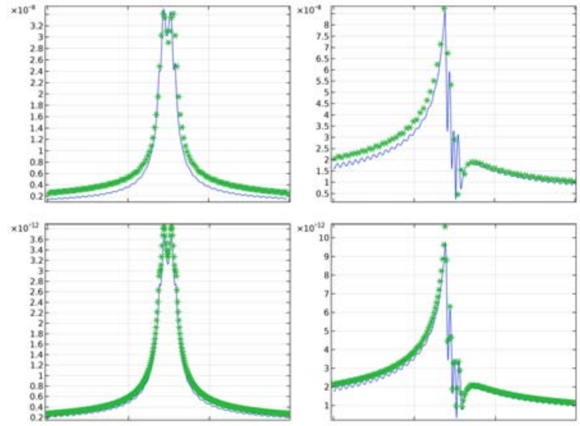

Figure 3. Comparison of the E_z field distribution calculated in native solver (green asterisk marker) and in Comsol (blue line) for the $\beta = 10^{-4}$ (at the top) and $\beta = 10^{-6}$ (at the bottom). Left side – along x axis, right side – along y axis.

Returning to Fig. 1, which was obtained specifically for these system parameters, we can state the following. In this specific case, the current densities depend only on two spatial coordinates (x and y), remaining constant along the cylinder's axis of symmetry (z). Moreover, the current component along this axis is strictly zero ($J_z = 0$), which slightly reduces the amount of data imported into COMSOL. Fig. 3 presents the validation results. The most notable is the secondary field component E_z, which is a second-order effect. The agreement between the results from the native solver and COMSOL is good. Possible sources of minor discrepancies include differences in solver fine-tuning, automatic mesh refinement during the solving process in COMSOL, and variations in post-processing algorithms. Both sets of results also cross-validate well against the analytical solution [1, 21].

5 Conclusion

An effective algorithm for integrating the recently developed BA methodology into the COMSOL Time Explicit EMW Module was presented, significantly enhancing its application potential in computational tasks. High accuracy in modeling complex medium effects was demonstrated. The presented validation confirms the approach's correctness. The results open up new opportunities for optimization and further development in numerical modeling of relevant problems. Additionally, partial verification of the approach was obtained for the classical 3D problem of scattering by a rotating sphere.

References

[1] M. Raffetto, M. R. Clemente Vargas, and K. Zeyde, “A new born-approximation approach to compute the effects of motion on the solution of electromagnetic problems involving moving materials with stationary boundaries,” *IET Science, Measurement & Technology*, **18**, 5, 2024, pp. 254–257.

[2] M. Raffetto and K. Zeyde, “First 3D results obtained by a new Born-approximation methodology for media in motion with stationary boundaries,” in *IEEE International Symposium on Antennas and Propagation and INC/USNC-URSI Radio Science Meeting (AP-S/INC-USNC-URSI)*, Firenze, Italy, 2024, pp. 1339–1340.

[3] K. M. Zeyde, V. V. Sharov, and M. V. Ronkin, “Guided microwaves electromagnetic drag over the sensitivity threshold experimental observation,” *WSEAS Transactions on Communications*, **18**, 2019, pp. 191–205.

[4] K. M. Zeyde, “Multiscale effects of continuous moving medium for the weak bianisotropy detection,” in *IEEE International Conference on Microwaves, Communications, Antennas, Biomedical Engineering and Electronic Systems (COMCAS)*, Tel-Aviv, Israel, 2024.

[5] Y. Yan, “Mass flow measurement of bulk solids in pneumatic pipelines,” *Meas. Sci. Technol.*, **7**, 12, 1996, pp. 1687–1706.

[6] K. M. Zeyde and I. B. Milochkin, “General algorithm for cognitive material measurements by the radio structuroscopy method,” in *5th International Conference on Control Systems, Mathematical Modeling, Automation and Energy Efficiency (SUMMA)*, Lipetsk, Russia, 2023, pp. 599–602.

[7] A. H. Sihvola, “Bi-isotropic mixture,” *IEEE Transactions on antennas and propagation*, **40**, 2, 1992, pp. 188–197.

[8] U. C. Hasar, J. J. Barroso, M. Bute, A. Muratoglu, and M. Ertugrul, “Boundary effects on the determination of electromagnetic properties of bianisotropic metamaterials from scattering parameters,” *IEEE Transactions on antennas and propagation*, **64**, 8, 2016, pp. 3459–3469.

[9] D. -L. Nguyen, “Direct and inverse electromagnetic scattering problems for bi-anisotropic media,” *Inverse problems*, **35**, 12, 2019, pp. 1340–1344.

[10] P. Kalarickel Ramakrishnan, M. R. Clemente Vargas, and M. Raffetto, “Electromagnetic inverse scattering of rotating axisymmetric objects,” *IEEE Access*, **9**, 2021.

[11] K. M. Zeyde, “Parameters specification of the 3D STEP object format in modular multiphysical modeling,” in *Ural Symposium on Biomedical Engineering, Radioelectronics and Information Technology (USBEREIT)*, Ekaterinburg, Russia, 2019, pp. 189–192.

[12] P. Kalarickel Ramakrishnan and M. Raffetto, “Well posedness and finite element approximability of three-dimensional time-harmonic electromagnetic problems involving rotating axisymmetric objects,” *Symmetry*, **12**, 2, 2020.

[13] G. Cevini, G. Oliveri, and M. Raffetto, “Further comments on the performances of finite element simulators for the solution of electromagnetic problems involving metamaterials,” *Microwave and Optical Technology Letters*, **48**, 12, 2006, pp. 2524–2529.

[14] D. K. Cheng and J. A. Kong, “Covariant descriptions of bianisotropic media,” *Proceedings of the IEEE*, **56**, 3, 1968, pp. 248–251.

[15] P. Fernandes, M. Ottonello, and M. Raffetto, “Regularity of time-harmonic electromagnetic fields in the interior of bianisotropic materials and metamaterials,” *IMA Journal of Applied Mathematics*, 79, 2014, pp. 54–93.

[16] P. Kalarickel Ramakrishnan and M. Raffetto, “Three-dimensional time-harmonic electromagnetic scattering problems from bianisotropic materials and metamaterials: reference solutions provided by converging finite element approximation,” *Electronics*, **9**, 7, 2020.

[17] K. Achouri and O. J. F. Martin, “Fundamental properties and classification of polarization converting bianisotropic metasurfaces,” *IEEE Transactions on antennas and propagation*, **69**, 9, 2021, pp. 5653–5663.

[18] J. D. Jackson, *Classical Electrodynamics*, 3rd ed. Wiley, New York, 1999.

[19] *RF Module User’s Guide, version 6.2*, COMSOL, Inc, www.comsol.com

[20] K. M. Zeyde, “The coordinate expression of the propagation constant for a moving dielectric medium,” in *Ural Symposium on Biomedical Engineering, Radioelectronics and Information Technology (USBEREIT)*, Ekaterinburg, Russia, 2018, pp. 295–298.

[21] C. Yeh, "Scattering obliquely incident microwaves by a moving plasma column," *Journal of Applied Physics*, **40**, 13, 1969, pp. 5066–5075.

[22] D. Censor, “Scattering of electromagnetic waves by a cylinder moving along its axis,” *IEEE Transactions on Microwave Theory and Techniques*, **MTT-17**, 3, 1969, 154–158.